Title

Phenolic Compounds Prevent Amyloid β-Protein Oligomerization and Synaptic Dysfunction by Site-specific Binding*

Journal

Journal of Biological Chemistry, 287(18)

ISSN

0021-9258

Authors

Ono, Kenjiro
Li, Lei
Takamura, Yusaku
et al.

Publication Date

2012-04-01

DOI

10.1074/jbc.m111.325456

Peer reviewed

THE JOURNAL OF BIOLOGICAL CHEMISTRY VOL. 287, NO. 18, pp. 14631–14643, April 27, 2012

Phenolic Compounds Prevent Amyloid β-Protein Oligomerization and Synaptic Dysfunction by Site-specific Binding*[S]

Received for publication, November 18, 2011, and in revised form, February 28, 2012 Published, JBC Papers in Press, March 5, 2012, DOI 10.1074/jbc.M111.325456

Kenjiro Ono[‡], Lei Li[§], Yusaku Takamura[¶], Yuji Yoshiike[‖], Lijun Zhu[§], Fang Han[§], Xian Mao[§], Tokuhei Ikeda[‡], Jun-ichi Takasaki[‡], Hisao Nishijo[¶], Akihiko Takashima[‖], David B. Teplow[**], Michael G. Zagorski[§1], and Masahito Yamada[‡2]

From the [‡]Department of Neurology and Neurobiology and Aging, Kanazawa University Graduate School of Medical Science, Kanazawa 920-8640, Japan, [§]Department of Chemistry, Case Western Reserve University, Cleveland, Ohio 44106, [¶]System Emotional Science, University of Toyama, Toyama 930-0194, Japan, the [‖]Laboratory for Alzheimer's Disease, Brain Science Institute, Riken, 2-1 Hirosawa, Wako, Saitama 351-0198, Japan, and [**]Department of Neurology and Mary S. Easton Center for Alzheimer's Disease Research at UCLA, David Geffen School of Medicine, and Molecular Biology Institute and Brain Research Institute, UCLA, Los Angeles, California 90095

Background: Epidemiological evidence suggests that consumption of phenolic compounds reduce the incidence of Alzheimer disease (AD).
Results: Myricetin and rosmarinic acid reduced cellular and synaptic toxicities by inhibition of amyloid β-protein (Aβ) oligomerization. Myricetin promoted NMR changes of Aβ.
Conclusion: Phenolic compounds are worthy therapeutic candidates for AD.
Significance: Phenolic compounds blocked early assembly processes of Aβ through differently binding.

Cerebral deposition of amyloid β protein (Aβ) is an invariant feature of Alzheimer disease (AD), and epidemiological evidence suggests that moderate consumption of foods enriched with phenolic compounds reduce the incidence of AD. We reported previously that the phenolic compounds myricetin (Myr) and rosmarinic acid (RA) inhibited Aβ aggregation *in vitro* and *in vivo*. To elucidate a mechanistic basis for these results, we analyzed the effects of five phenolic compounds in the Aβ aggregation process and in oligomer-induced synaptic toxicities. We now report that the phenolic compounds blocked Aβ oligomerization, and Myr promoted significant NMR chemical shift changes of monomeric Aβ. Both Myr and RA reduced cellular toxicity and synaptic dysfunction of the Aβ oligomers. These results suggest that Myr and RA may play key roles in blocking the toxicity and early assembly processes associated with Aβ through different binding.

Alzheimer disease (AD)[3] has been characterized historically by the accumulation of intraneuronal filaments formed by the microtubule-associated protein Tau and of extracellular parenchymal and vascular amyloid deposits largely comprising the amyloid β protein (Aβ) (1). Continuing investigations of the pathogenetic relationships among Tau, Aβ, and AD suggest that oligomeric forms of Aβ play a seminal role in disease causation (1, 2). More recent evidence suggests that low *n*-order oligomers are especially important (3). Townsend *et al.* (4) found that Aβ trimers fully inhibit long term potentiation, whereas dimers and tetramers have an intermediate potency. Dimers and trimers from the conditioned medium of amyloid precursor protein-expressing CHO cells have been found to cause progressive loss of synapses in organotypic rat hippocampal slices (5). Aβ oligomers extracted from AD brains disrupt synaptic function, and dimers were the smallest oligomers showing activity (6). Recently, structure-cytotoxicity studies of pure Aβ oligomer populations produced the first determinations of oligomer-specific activity (7), in that dimers, trimers, and tetramers all were significantly more toxic than monomers. Importantly, a non-linear dependence of cytotoxicity on oligomer order was observed. Thus, the most efficacious therapeutic agents should perhaps target monomeric Aβ and prevent its assembly into any sized oligomer (3).

* This work was supported by Grants-in-aid for Young Scientists (B) (to K. O.), Scientific Research (A) (22240051) (to H. N.), Scientific Research (B) (20390242) (to M. Y.), and Knowledge Cluster Initiative (High Tech Sensing and Knowledge Handling Technology (Brain Technology)) (to M. Y.) from the Japanese Ministry of Education, Culture, Sports, Science, and Technology, a grant to the Amyloidosis Research Committee from the Ministry of Health, Labor, and Welfare (Japan) (to K. O. and M. Y.), Novartis Foundation for Gerontological Research (to K. O.), Alumni Association of Showa University School of Medicine (to K. O.), Japan Society for the Promotion of Science Asian Core Program (to H. N.), and National Institutes of Health Grants AG027818 (to D. B. T.) and AG027853 (to M. G. Z.), and the Jim Easton Consortium for Alzheimer Drug Discovery and Biomarkers at UCLA (to D. B. T.).
[S] This article contains supplemental Table S1 and Figs. S1–S7.
[1] To whom correspondence may be addressed: Dept. of Chemistry, Case Western Reserve University, Cleveland, OH 44106. Tel.: 1-216-368-3706; Fax: 1-216-368-3006; E-mail: michael.zagorski@case.edu.
[2] To whom correspondence may be addressed: Dept. of Neurology and Neurobiology of Aging, Kanazawa University Graduate School of Medical Science, Kanazawa 920-8640, Japan. Tel.: 81-76-265-2290; Fax: 81-76-234-4253; E-mail: m-yamada@med.kanazawa-u.ac.jp.

[3] The abbreviations used are: AD, Alzheimer disease; Aβ, amyloid β-protein; AFM, atomic force microscopy; Cur, curcumin; FA, ferulic acid; fAβ, Aβ fibrils; fEPSP, field excitatory presynaptic potential; HSQC, heteronuclear single quantum coherence; LTD, long term depression; LTP, long term potentiation; MTT, 3-(19)-2,5-diphenyltetrazolium bromide; Myr, myricetin; NDGA, nordihydroguaiaretic acid; PICUP, photo-induced cross-linking of unmodified proteins; RA, rosmarinic acid; Ru(bpy), tris(2,2′-bipyridyl)dichlororuthenium(II); STD, saturation transfer difference.

Nature itself may have created useful therapeutic agents of AD. The relevance of this finding to AD has come from French and Danish epidemiological studies suggesting that moderate wine drinking may protect against AD (8, 9). Investigation of this phenomenon may reveal the answer for the protective effects of wine against AD. Classical biochemical fractionation studies have shown that the active components of red wine are phenolic compounds, including resveratrol and the proanthocyanidins (10). Resveratrol was found to lower significantly the levels of secreted and intracellular Aβ produced in a variety of cell lines by increasing proteasome-mediated Aβ degradation (11). Interestingly, a related polyphenolic compound, curcumin (Cur), is found in the common spice curry (12). As with red wine, epidemiologic studies have shown a correlation between curry consumption and decreased AD risk (13). The concordance of results from these different systems emphasizes the potential importance of elucidating the mechanism through which phenolic compounds may alter Aβ aggregation and toxicity.

Initial mechanistic studies have focused on formation of large aggregates, Aβ fibrils (fAβ). Phenolic compounds, such as the wine-related polyphenol myricetin (Myr), a major component of curry spice turmeric Cur, its analog rosmarinic acid (RA), nordihydroguaiaretic acid (NDGA), and ferulic acid (FA) inhibit the formation of fAβ as well as dissociate preformed fibrils by preferentially and reversibly binding to these structures (14–16). In cell culture experiments, Myr-treated fAβ were less toxic than intact fAβ (14). Recently, a commercially available grape seed polyphenolic extract, MegaNatural®, was shown to inhibit significantly the aggregation of Aβ into SDS-stable high molecular weight oligomers (15–20 monomers) using AD model transgenic animals (Tg2576) (17). We showed that the phenolic compounds such as Myr, Cur, and RA prevented the development of AD pathology and reduced high molecular weight oligomers in Tg2576 mice (18).

In the studies reported here, we sought to determine how the phenolic compounds affected Aβ conformational dynamics and the early stages of Aβ assembly. To do so, we analyzed the assembly of the Aβ42 and Aβ40 with five phenolic compounds, Myr, FA, NDGA, Cur, and RA (Fig. 1) using several well established techniques for studying amyloid formation, including photo-induced cross-linking of unmodified proteins (PICUP), atomic force microscopy (AFM), circular dichroism (CD) spectroscopy, and nuclear magnetic resonance (NMR). Next, we examined whether the phenolic compounds reduced Aβ assembly-induced cytotoxicity and synaptic dysfunction using 3-(19)-2,5-diphenyltetrazolium bromide (MTT) assays and electrophysiological assays for long term potentiation (LTP) and depression (LTD) in hippocampal slices.

EXPERIMENTAL PROCEDURES

Chemicals and Reagents—Chemicals were obtained from Sigma-Aldrich and were of the highest purity available. Water was produced using a Milli-Q system (Nihon Millipore K.K.).

Proteins and Phenolic Compounds—Aβ peptides were synthesized, purified, and characterized as described previously (20, 21). Briefly, synthesis was performed on an automated peptide synthesizer (model 433A, Applied Biosystems) using 9-fluorenylmethoxycarbonyl-based methods on pre-loaded Wang resins. Peptides were purified using reverse-phase HPLC. Quantitative amino acid analysis and mass spectrometry yielded the expected compositions and molecular weights, respectively, for each peptide. Purified peptides were stored as lyophilizates at −20 °C. [Met(O)^{35}]Aβ42 peptide was purchased from Bachem AG (Bubendorf, Switzerland). To prepare peptides for study, Aβ peptide lyophilizates were dissolved at a nominal concentration of 25 or 50 μM in 10% (v/v) 60 mM NaOH and 90% (v/v) 10 mM phosphate buffer, pH 7.4. After sonication for 1 min, the peptide solution was centrifuged for 10 min at 16,000 × *g*. A stock solution of GST (Sigma-Aldrich) was prepared by dissolving the lyophilizate to a concentration of 250 μM in 60 mM NaOH. Prior to use, aliquots were diluted 10-fold into 10 mM sodium phosphate, pH 7.4. We examined 5-phenolic compounds such as Myr, FA, NDGA, Cur, and RA. They were dissolved in ethanol to a final concentration of 2.5 mM and then diluted with 10 mM phosphate, pH 7.4, to produce concentrations of 5, 10, 25, 50, 100, and 500 μM for CD, PICUP, and AFM, as described previously (20).

CD—CD spectra of Aβ:compound mixtures were acquired immediately after sample preparation or following 2, 3, 5, or 6 days of incubation. CD measurements were made by removing a 200-μl aliquot from the reaction mixture, adding the aliquot to a 1-mm path length CD cuvette (Hellma, Forest Hills, NY), and acquiring spectra in a J-805 spectropolarimeter (JASCO). The CD cuvettes were maintained on ice prior to introduction into the spectrometer. Following temperature equilibration, spectra were recorded at 22 °C from ~190–260 nm at 0.2 nm resolution with a scan rate of 100 nm/min. Ten scans were acquired and averaged for each sample. Raw data were manipulated by smoothing and subtraction of buffer spectra according to the manufacturer's instructions.

Chemical Cross-linking and Determination of Oligomer Frequency Distributions—Immediately after their preparation, samples were cross-linked using PICUP, as described (22). Briefly, to 18 μl of 50 μM protein solution were added 1 μl of 4 mM tris(2,2′-bipyridyl)dichlororuthenium(II) (Ru(bpy)) and 1 μl of 80 mM ammonium persulfate. The final protein:Ru(bpy):ammonium persulfate molar ratios of Aβ40 or Aβ42 was 1:4:80. The mixture was irradiated for 1 s with visible light, and then the reaction was quenched with 2 μl of 1 M DTT (Invitrogen) in ultrapure water. Determination of the frequency distribution of monomers and oligomers was accomplished using SDS-PAGE and silver staining as described (22). Briefly, 8 μl of each cross-linked sample was electrophoresed on a 10–20% gradient tricine gel and visualized by silver staining (Invitrogen). Uncross-linked samples were used as controls in each experiment. Densitometry was performed with a luminescent image analyzer (LAS 4000 mini, Fujifilm, Tokyo, Japan) and image analysis software (Multi gauge, version 3.2., Fujifilm). The intensity of each band in a lane from the SDS gel was normalized to the sum of the intensities of all the bands in that lane, according to the formula, $R_i = I_i/\Sigma_{i=1}^{n} I_i \times 100$ (%), where R_i is the normalized intensity of band *I*, and I_i is the intensity of each band *i*. R_i varies from 0–100. To calculate the oligomer ratio, the sum of oligomers intensities of Aβ40 or Aβ42 with 5, 10, 25, 50, 100, and 500 μM Myr, FA, NDGA, Cur, or RA, respectively, was divided by

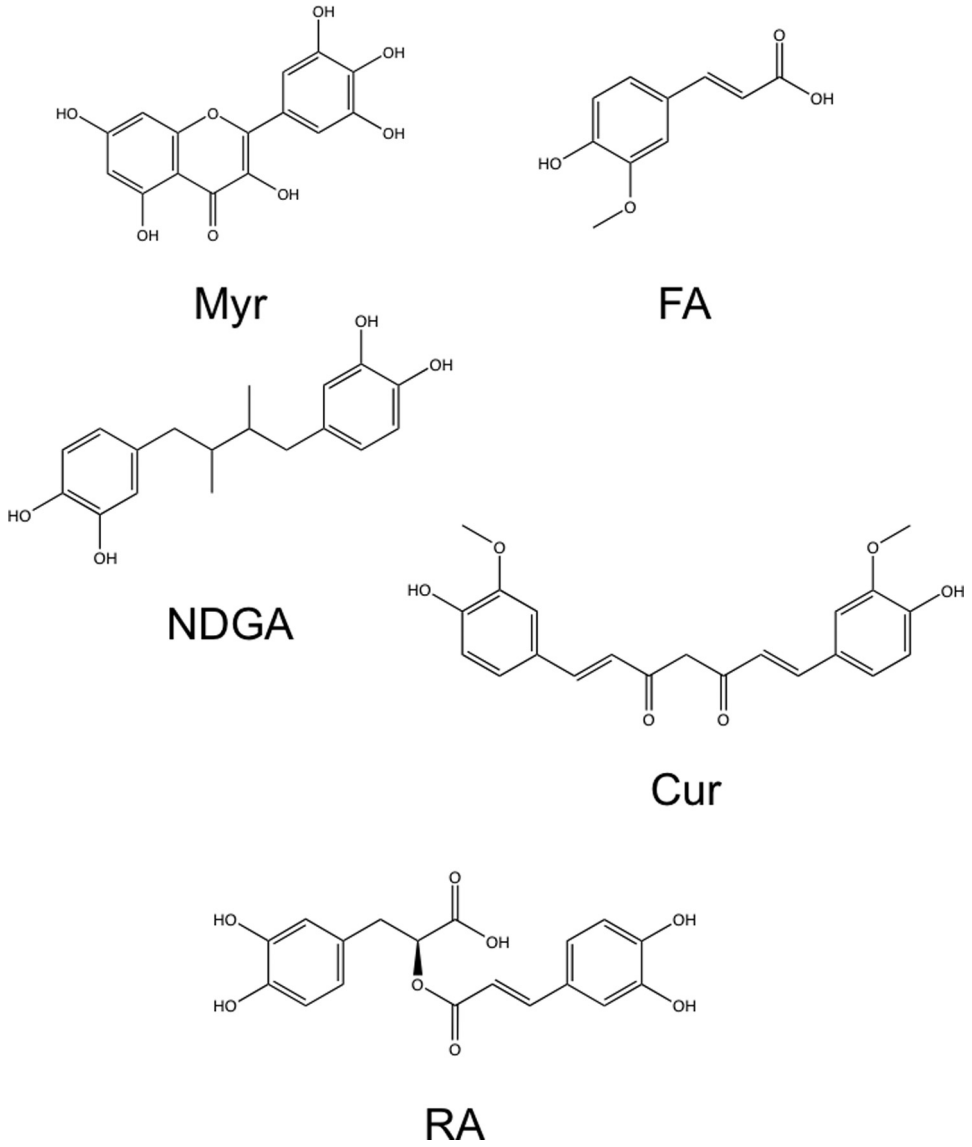

FIGURE 1. **Structures of Myr, FA, NDGA, Cur, and RA.**

the sum of oligomer intensities without each compound. The EC_{50} was defined as the concentration of Mel to inhibit α-synuclein oligomerization to 50% of the control value. EC_{50} was calculated by sigmoidal curve fitting, using GraphPad Prism software (version 4.0a, GraphPad Software, Inc.).

Size-exclusion Chromatography—PICUP reagents and phenolic compounds were removed from cross-linked samples by size-exclusion chromatography as described previously (23). To do so, 1.5-cm diameter cylindrical columns were packed manually with 2 g of Bio-Gel P2 Fine (Bio-Rad Laboratories), which produced a 6-ml column volume. The column first was washed twice with 25 ml of 50 mM NH_4HCO_3, pH 8.5. Two hundred sixteen μl of cross-linked sample was then loaded. The column was eluted with the same buffer at a flow rate of ≈ 0.15 ml/min. The first 1 ml of eluate was collected. The fractionation range of the Bio-Gel P2 column is 100–1800 Da. Aβ peptides thus elute in the void volume, whereas Ru(bpy) (MW = 748.6), ammonium persulfate (MW = 228.2), Myr (MW = 318.2), RA (MW = 360.3), and DTT (MW = 154.2) enter the column matrix and are separated from Aβ.

Fractions were lyophilized immediately after collection. Reconstitution of the lyophilizates to a nominal concentration of 25 μM in 10 mM sodium phosphate, pH 7.4, followed by SDS-PAGE analysis, showed that removal of reagents and phenolic compounds, lyophilization, and reconstitution did not alter the oligomer composition of any of the peptide populations under study (supplemental Fig. S1).

AFM—Peptide solutions were characterized using a Nanoscope IIIa controller (Veeco Digital Instruments) with a multimode scanning probe microscope equipped with a JV scanner. All measurements were carried out in the tapping mode under ambient conditions using single-beam silicon cantilever probes. A 10-μl aliquot of each peptide lyophilizate, reconstituted to a concentration of 25 μM in 10 mM PBS, pH 7.4, was spotted onto freshly cleaved mica (Ted Pella, Inc.), incubated at room temperature for 5 min, rinsed with water, and then blown dry with air. At least four regions of the mica surface were examined to confirm the homogeneity of the structures throughout the sample. Mean particle heights were analyzed by averaging the measures values of eight individual cross-sec-

tional line scans from each image only when the particle structure was confirmed.

NMR Spectroscopy—Stock solutions of the five phenolic compounds (2.5 mM), and monomeric, uniformly ^{15}N-labeled Aβ42 peptide (0.25 mM) (rPeptide) and Aβ40 (0.25 mM) were prepared by dissolution (with sonication) in aqueous basic solution (pD 11, 1 ml, 10 mM NaOD) (21). Aliquots of the Aβ42 and phenolic solutions were combined and mixed with cold (5 °C) phosphate buffer solution (0.5–1.0 ml, 5 mM, pH 7.5) that contained 0.5 mM predeuterated ethylenediamine tetraacetic acid (Na_2EDTA-d_{12}), and 0.05 mM NaN_3. The aliquots were varied so that the final peptide:compound concentration ratio was 25:500 μM. To prevent aggregation, peptide solutions were kept cold (5 °C), and standard ^{1}H-^{15}N heteronuclear single quantum coherence (HSQC) spectra were obtained within 30 min of the sample preparation. Spectra were obtained at 5 °C with a Bruker Avance-II 900 MHz spectrometer equipped with a TXI cryoprobe (Bruker BioSpin, Inc.).

The saturation transfer difference (STD) experiments were obtained with the Aβ40 (25 μM) alone or with RA or Myr (50 μM) at pH 7.5 and 5 °C. Data were acquired at 900.18 MHz using the pulse program (selective irradiation)-(non selective excitation)-(watergate)-(acquisition) (24, 25). The selective irradiation used a 3.9-s long and weak pulse that was alternatively applied at -0.2 ppm (where there was a peak) and at 30 ppm (where there was no peak), the latter constituting the reference spectra. The non-selective excitation was achieved with a 90° pulse at the water position (4.7 ppm), and the Watergate 3-9-19 pulse sequence was used to suppress the water signal. Each spectrum was acquired with 128 scans (12 min) and stored separately. The STD was obtained by subtracting the reference spectra from that obtained with irradiation at −0.2 ppm. All NMR spectra were processed with the NMRPipe (26), Mnova, or CARA programs using a PC computer.

NMR-based Molecular Modeling—Atomic coordinates of the NMR/molecular dynamics Aβ42 structural model were kindly provided by Dr. Chunyu Wang (Rensselaer Polytechnic Institute) (27). With the model, the regions showing the most pronounced NH chemical shift movements (>0.02 ppm) were revealed using the Swiss PDB Viewer program (28). These (backbone) regions were labeled with *red* and the regions not showing movement with *green*.

Cell Culture—HEK 293 cells were cultured in 75-cm^2 flasks (Corning, Inc.) in DMEM (Sigma-Aldrich) containing 10% fetal bovine serum and incubated in a humidified chamber (85% humidity) containing 5% CO_2 at 37 °C. One day before peptide sample treatment, the cell culture medium was replaced with serum-free DMEM, and the cells were trypsinized and replated onto coated 96-well plates at a final cell density of 20,000 cells/well.

Cytotoxicity Assays—We used to test the toxicity of uncross-linked, cross-linked, cross-linked with Myr, and cross-linked with RA of Aβ42 as assessed in MTT assay. Peptide samples were prepared at Aβ concentrations of 2 and 20 μM in 10 mM sodium phosphate, pH 7.4. Aliquots of 50 μl were added to HEK cells to yield final Aβ concentrations of 1 and 10 μM. Twenty hours after the cells were incubated with peptide samples, MTT was added to each well, and the plates were kept in a CO_2 incubator for an additional 2 h. The cells were then lysed by adding lysis solution (50% dimethylformamide, 20% SDS at pH 4.7) and were incubated overnight. The degree of MTT reduction (*i.e.* cell viability) in each sample was subsequently assessed by measuring absorption at 590 nm at room temperature using a plate reader (PerkinElmer, Turku, Finland). Controls included medium with sodium phosphate ("negative") and 1 μM poly-L-lysine (average MW, 75,000 Da) (Sigma-Aldrich) ("maximal positive"). Background absorbance values, as assessed from cell-free wells, were subtracted from the absorption values of each test sample. The absorbance measured from the three wells were averaged and reported as mean ± S.E. percentage of cell viability,

$$V = 100 - ((A_{A\beta} - A_{medium})/(A_{poly\text{-}L\text{-}lysine} - A_{medium})) \times 100 \quad \text{(Eq. 1)}$$

where $A_{A\beta}$, A_{medium}, and $A_{poly\text{-}L\text{-}LYSINE}$ were absorbance values from Aβ-containing samples, medium alone, or poly-L-lysine alone, respectively.

Electrophysiology—The field excitatory postsynaptic potentials (fEPSPs) were recorded from the CA1 region of acute hippocampal slices derived from C57BL/6 mice (male, 4–5 weeks of age). The procedures for slice preparation and electrophysiological recording were described previously (29). Briefly, 300-μm thick transverse hippocampal slices were placed in a physiological chamber perfused with artificial cerebrospinal fluid (125 mM NaCl, 3.5 mM KCl, 1.25 mM NaH_2PO_4, 25 mM $NaHCO_3$, 2.0 mM $MgSO_4$, 2.0 mM $CaCl_2$, and 20 mM glucose and aerated with a mixture of 95% O_2 and 5% CO_2) at a rate of 1 ml/min at 30 °C. Shaffer collaterals/commissural bundle in the CA3 hippocampal subfield were stimulated using a bipolar stainless steel wire electrode at 20-s intervals throughout the experiment. The fEPSPs were recorded from the stratum radiatum in the CA1 hippocampal subfield using a sharp glass electrode (2–6 megohms, filled with 2 M NaCl). LTP was induced by tetanic stimulation delivered at 100 Hz for 1 s. LTD was induced by low frequency 450 paired-pulse stimulation (50 ms paired-pulse interval, 1 Hz) for 7.5 min. LTD was induced only under the presence of cross-linked Aβ42 oligomer in this condition (see "Results"). Each Aβ42 sample (500 nM in 0.3 mM NaOH in artificial cerebrospinal fluid) or vehicle (0.3 mM NaOH in artificial cerebrospinal fluid) was applied for 20 min so that Aβ42 sample/vehicle application overlapped and coterminated with conditioning stimulation for LTP or LTD. The evoked potential was amplified (×1000), filtered (0.1–1000 Hz), digitized (20 kHz), and stored in a computer for off-line analysis using the PowerLab system (AD Instruments, Colorado Springs, CO). LTP and LTD values were presented as the percentage of average fEPSPs slope relative to the mean value of the base line before conditioning stimulation.

Statistical Analysis—One-way factorial analysis of variance followed by Tukey-Kramer post hoc comparisons were used to determine statistical significance among data sets. These tests were implemented within GraphPad Prism software (GraphPad Software). Significance was defined as $p < 0.05$.

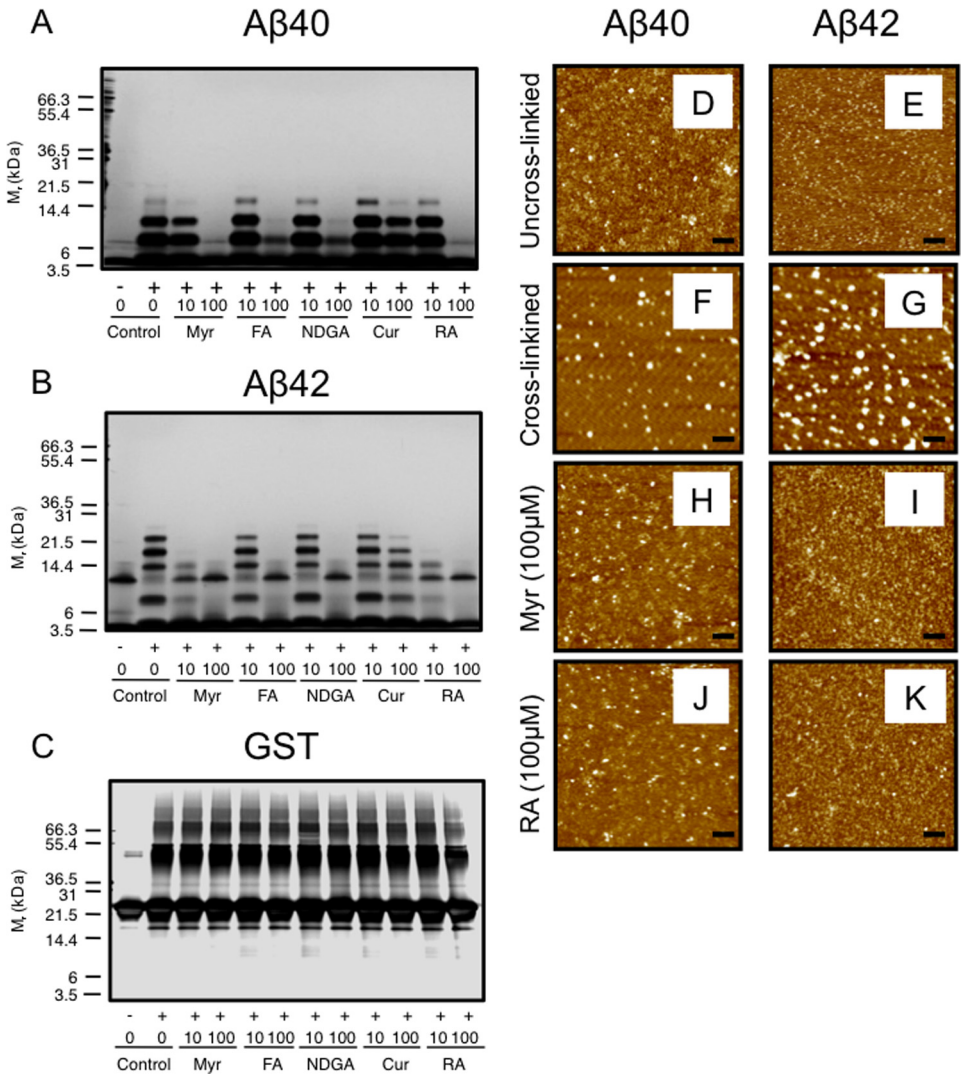

FIGURE 2. **Aβ and GST oligomerizations.** PICUP, followed by SDS-PAGE and silver staining, was used to determine the effects of 10 and 100 μM Myr, FA, NDGA, Cur, or RA on oligomerization of Aβ40 (*A*), Aβ42 (*B*), or GST (*C*). +, with cross-linking; −, without cross-linking. The gel is representative of each of three independent experiments. AFM was performed on 25 μM uncross-linked (*D* and *E*) and cross-linked (*F–K*) Aβ40 (*D*, *F*, *H*, and *J*) and Aβ42 (*E*, *G*, *I*, and *K*) with 0 (*F* and *G*), 100 μM Myr (*H* and *I*) or RA (*J* and *K*). *Scale bars* are 100 nm.

RESULTS

Aβ Oligomerization—To determine whether the five phenolic compounds blocked formation of low *n*-order Aβ oligomers, we used PICUP, a photochemical cross-linking method that is rapid, efficient, requires no structural modification of Aβ, and accurately reveals the oligomerization state of Aβ (22). In the absence of cross-linking, only Aβ40 monomers (Fig. 2*A*) and Aβ42 monomers and trimers (Fig. 2*B*) were observed. The Aβ42 trimer band has been shown to be an SDS-induced artifact (22). Following cross-linking and as reported previously (22), Aβ40 existed predominately as a mixture of monomers and oligomers of order 2–4 (Fig. 2*A*), whereas Aβ42 comprised predominately monomers and oligomers of order 2–6 (Fig. 2*B*).

When 10 μM Myr was mixed with Aβ40 at a peptide:compound ratio of 5:2, oligomerization was blocked slightly (Fig. 2*A*). The intensity of tetramer band was decreased. When 100 μM Myr was mixed with Aβ40 at a peptide:compound ratio of 1:4, oligomerization was blocked almost completely (Fig. 2*A*). The effect of Myr on Aβ42 oligomerization was equally significant (Fig. 2*B*). When 10 μM Myr was mixed with Aβ42 at a peptide:compound ratio of 5:2, oligomerization was blocked moderately. The pentamer and hexamer bands disappeared, and the intensity of tetramer band markedly decreased (Fig. 2*B*). At peptide:compound ratio of 1:4, Myr produced oligomer distributions almost identical to those of untreated Aβ42, consistent with an essentially complete inhibition of oligomerization (Fig. 2*B*). When 10 or 100 μM RA was mixed with Aβ40 or Aβ42 at the same ratios as used above, comparable effects were observed on Aβ oligomerization (Fig. 2, *A* and *B*).

With Aβ40:FA at a 5:2 ratio, no inhibition of oligomerization was observed (Fig. 2*A*). At a higher concentration of FA (Aβ40:FA, 1:4), the trimer and tetramer bands disappeared, and the intensity of dimer band decreased (Fig. 2*A*). Similarly, with Aβ42:FA at a 5:2 ratio, no inhibition of the oligomerization was observed (Fig. 2*B*), whereas at higher concentration of FA (Aβ42:FA, 1:4), the pentamer and hexamer bands disappeared, and the intensity of tetramer band weakened (Fig. 2*B*). When 10

or 100 μM NDGA was mixed with Aβ40 or Aβ42, similar strong effects was observed on Aβ oligomerization (Fig. 2, *A* and *B*).

When 10 μM Cur was mixed with Aβ40 at a peptide:compound ratio of 5:2, no inhibition of oligomerization was observed (Fig. 2*A*). When 100 μM Cur was mixed with Aβ40 at a peptide:compound ratio of 1:4, oligomerization was blocked slightly (Fig. 2*A*). The intensity of tetramer band was decreased slightly. Similarly, when 10 μM Cur was mixed with Aβ42 at a peptide:compound ratio of 5:2, no inhibition of oligomerization was observed (Fig. 2*B*). At higher concentration of Cur (Aβ42: Cur, 1:4), oligomerization was blocked slightly (Fig. 2*B*). The intensities of dimer, pentamer, and hexamer band were decreased slightly.

We confirmed dose dependence of these inhibitions (supplemental Fig. S2). The effective concentrations (EC_{50}) of Myr, FA, NDGA, Cur, and RA for the Aβ40 oligomerization were 12.4, 76.2, 34.5, 60.8, and 25.6 μM, respectively. The effective concentrations (EC_{50}) of Myr, FA, NDGA, Cur, and RA for the Aβ42 oligomerization were 7.0, 52.6, 38.3, 108.2, and 10.8 μM, respectively. Taken together, the data indicate that inhibitory activity of Aβ40 and Aβ42 oligomerization by the phenolic compounds examined in this study may be in the following order: Myr > RA > NDGA = FA ≥ Cur.

In the absence of cross-linking, only [Met(O)^{35}]Aβ42 monomers were observed (supplemental Fig. S3). Following cross-linking, and as reported previously (30), [Met(O)^{35}]Aβ42 existed predominately as a mixture of monomers and oligomers of order 2–5 (supplemental Fig. S3). When 10 or 100 μM Myr was mixed with [Met(O)^{35}]Aβ42, oligomerization was blocked significantly (supplemental Fig. S3). The intensity of trimer, tetramer, and pentamer bands disappeared, and the intensity of dimer band markedly decreased. Similar effects were observed when 10 or 100 μM RA was mixed with [Met(O)^{35}]Aβ42 (supplemental Fig. S3).

A potential problem relates to the possibility that the strong inhibition of Aβ oligomerization could have resulted from an alternative compound, which may form from a possible side reaction of the inhibitor and the PICUP sensitizer. To evaluate this possibility, cross-linking reactions also were performed on glutathione *S*-transferase (GST; ~26 kDa), a positive control for the cross-linking chemistry (31). Uncross-linked GST exhibited an intense monomer band and a relatively faint dimer band (Fig. 2*C*). Cross-linking produced an intense dimer band, which was expected because GST exists normally as a homodimer, as well as higher-order cross-linked species. No alterations in GST cross-linking were observed in the presence of Myr, FA, NDGA, Cur, or RA at either of the two protein: compound ratios tested, 5:2 or 1:4 (Fig. 2*C*). Thus, the significant inhibition of Aβ40 and Aβ42 oligomerization is from a direct interaction with the phenolic compounds.

Aβ Assembly Morphology—To determine the morphology of the small assemblies present following PICUP of Aβ40 and Aβ42 with or without phenolic compounds, we used AFM. The height of uncross-linked Aβ40 was 0.23 ± 0.03 nm (Fig. 2*D* and supplemental Table S1). Following PICUP, the height of Aβ40 oligomers became 0.90 ± 0.05 nm (Fig. 2*F* and supplemental Table S1). The height of uncross-linked Aβ42 was 0.33 ± 0.02 nm (Fig. 2*E* and supplemental Table S1). Following PICUP, the height of Aβ42 oligomers became 1.39 ± 0.09 nm (Fig. 2*G* and supplemental Table S1). These morphologies are not inconsistent with our previous findings (7, 23). When Aβ40 was cross-linked with Myr at a compound:peptide ratio of 4:1, the height of treated Aβ40 decreased to 0.32 ± 0.03 nm (Fig. 2*H* and supplemental Table S1). When Aβ40 was cross-linked with RA at a compound:peptide ratio of 4:1, the height of treated Aβ40 decreased to 0.42 ± 0.04 nm (Fig. 2*J* and supplemental Table S1). Similarly, when Aβ42 was cross-linked with Myr or RA at a compound:peptide ratio of 4:1, the height of treated Aβ40 decreased clearly (Fig. 2, *I* and *K*, and supplemental Table S1).

Aβ Secondary Structure Dynamics—The above oligomerization studies revealed effects of the phenolic compounds at the initial stages of peptide self-association. To examine whether the phenolic compounds altered the secondary structure of the Aβ, we undertook CD studies (Fig. 3). Aβ40 and Aβ42, incubated alone, produced initial spectra characteristic of statistical coils (Fig. 3, *A* and *B*). The major feature of these spectra was a large magnitude minimum centered at ~198 nm. Aβ40 displayed substantial secondary structure changes between days 3–5 that were consistent with previously reported statistical coils → α-helix/β-sheet → β-sheet transitions associated with monomer → protofibril → fibril assembly (20). The Aβ42 system displayed similar structural changes, although, as expected, these changes occurred at much faster rate (0–2 days). When Aβ40 or Aβ42 were incubated with Myr at a compound:peptide ratio of 4:1, no such transitions were observed (Fig. 3, *C* and *D*). Similarly, no such transitions were observed in the presence of RA (Fig. 3, *E* and *F*). All spectra of Aβ40 and Aβ42 treated by Myr or RA revealed populations of conformers that were largely statistical coils.

NMR Studies—The binding between the phenolic compounds and Aβ42 was explored using NMR spectroscopy, a well accepted tool for obtaining atomic level aspects of protein structure and ligand binding. The sample preparation protocol and lower NMR probe temperature (5 °C) ensured that the Aβ42 remained monomeric during the entire data acquisition period (21, 32). Standard HSQC spectra were obtained with uniformly ^{15}N-labeled Aβ42, and the compound:peptide was kept at a 20:1 molar ratio. The HSQC experiment detects ^{1}H signals that are directly bonded to the ^{15}N atoms and thus provides a fingerprint of the amide-NH backbone atoms. In the present study, the HSQC data demonstrate that the phenolic compounds do not induce AβMet-35^{red} → AβMet-35^{ox} oxidation (21).

Shown in Fig. 4 are superimposed HSQC spectra of the Aβ42 alone (*black cross-peaks*) and the Aβ42 containing RA (Fig. 4*A*, *red cross-peaks*) and Myr (Fig. 4*B*, *red cross-peaks*). Because the cross-peaks of the superimposed spectra in Fig. 4*A* coincide, this indicates that RA does not bind with monomeric Aβ42. By contrast, the HSQC spectra with Myr show pronounced NH chemical shift movements (labeled peaks in Fig. 4*B*) indicative of binding. The most pronounced movements (0.02–0.05 ppm) were in the ^{1}H dimension and were among the Arg-5, Val-12, His-13, Lys-16, Leu-17, Val-18, Phe-19, Phe-20, Ala-21, Glu-23, Asp-23, Ile-31, and Ile-32 residues. In addition to movement, NH peak broadening occurred with Arg-5, Val-12, Lys-16, and Val-18, suggesting that the binding may be stronger with these

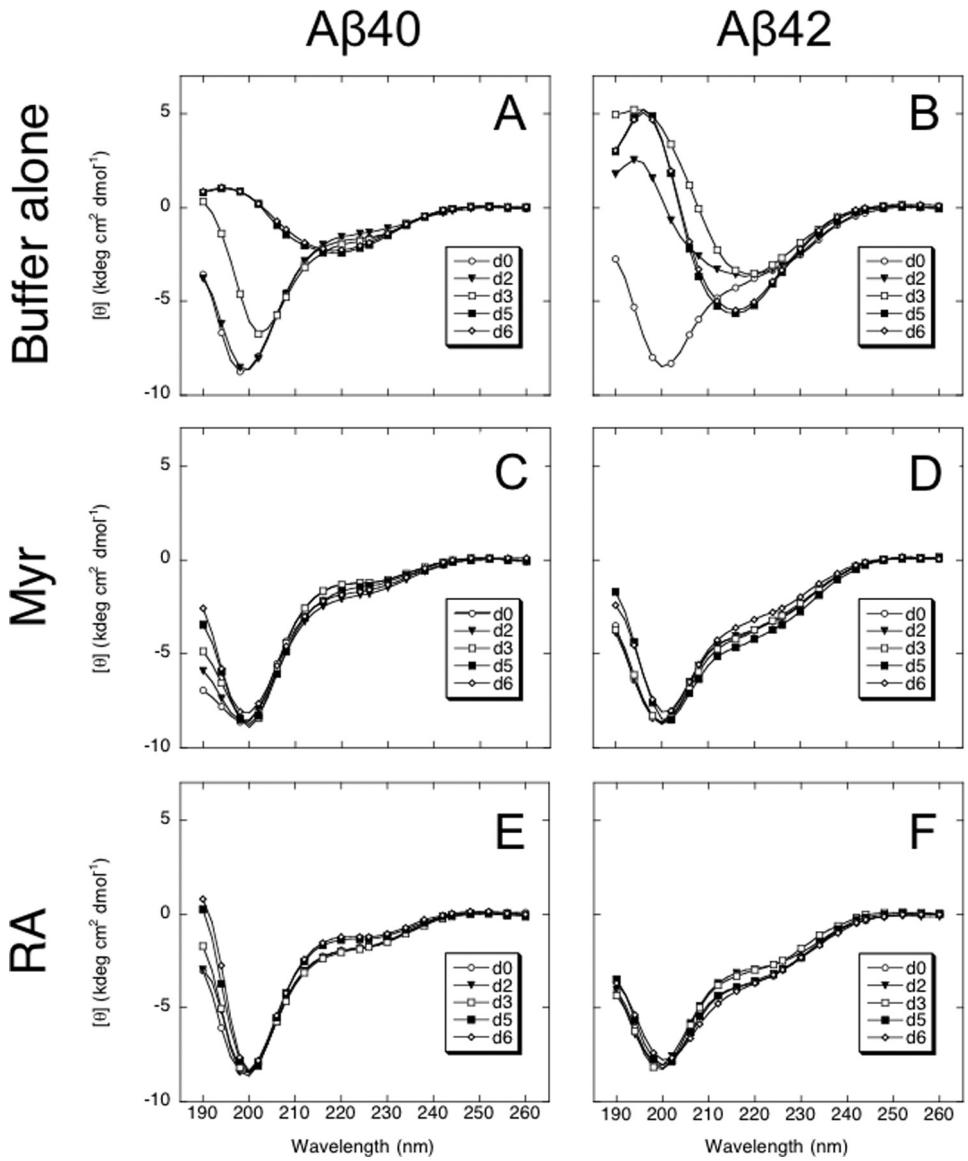

FIGURE 3. **Aβ secondary structure dynamics.** CD was used to monitor peptide assembly. Aβ40 (*A*, *C*, and *E*) or Aβ42 (*B*, *D*, and *F*) were incubated at 37 °C for 6 days in 10 mM phosphate, pH 7.4, in buffer alone (*A* and *B*) or in the presence of 100 μM Myr (*C* and *D*) or RA (*E* and *F*). Spectra were acquired immediately at the start of the incubation period, day 0 (○), and after days 2 (▼), 3 (□), 5 (■), and 6 (◇). The spectra presented at each time are representative of those obtained during each of three independent experiments. *deg*, degree.

residues. Less peak movements were seen with FA, NDGA, and Cur and were not localized to any specific peptide region (supplemental Fig. S4).

The binding of RA and Myr were further explored using STD experiments, which is a well established homonuclear NMR technique that permits detection of transient binding of small molecule ligands to macromolecular receptors. Notably, the STD has been used to discriminate ligand binding to monomeric or oligomeric states of the Aβ that co-exist in solution (24, 33, 34). In the STD, two separate spectra are obtained and then subtracted, where one spectra involves saturation of a resonance that belongs to the receptor (in this case the Aβ), whereas the second spectra involves saturation in a far-removed region that does not contain signals. The presence and strength of signals in the STD is indicative of binding.

Shown in supplemental Fig. S5 are three groups of spectral data: Aβ40 alone (supplemental Fig. S5, *A* and *B*), Aβ40 with RA (supplemental Fig. S5, *C* and *D*), and Aβ40 with Myr (supplemental Fig. S5, *E* and *F*). As expected, the STD spectra of Aβ40 alone (supplemental Fig. S5*B*) has no signals. In contrast, spectra containing RA (supplemental Fig. S5*D*) has extremely weak, barely discernable peaks, whereas that containing Myr (supplemental Fig. S5*F*) has obvious peaks. Because solution NMR detects only monomeric Aβ (21, 24), these data demonstrate that Myr binds to monomeric Aβ, whereas RA does not bind or binds very weakly. Overall, these results are consistent with the above HSQC data.

Highlighted in Fig. 5 are molecular models of the Aβ42 that were obtained from a combined molecular dynamics and NMR approach (27). In solution, the Aβ42 adopts a rapidly equilibrating ensemble of conformations, which, for the monomeric aggregation state are unstructured predominately (21, 32). These models effectively depict a single, highly populated conformation that has β-hairpin at residues Ile-31–Leu-34 and

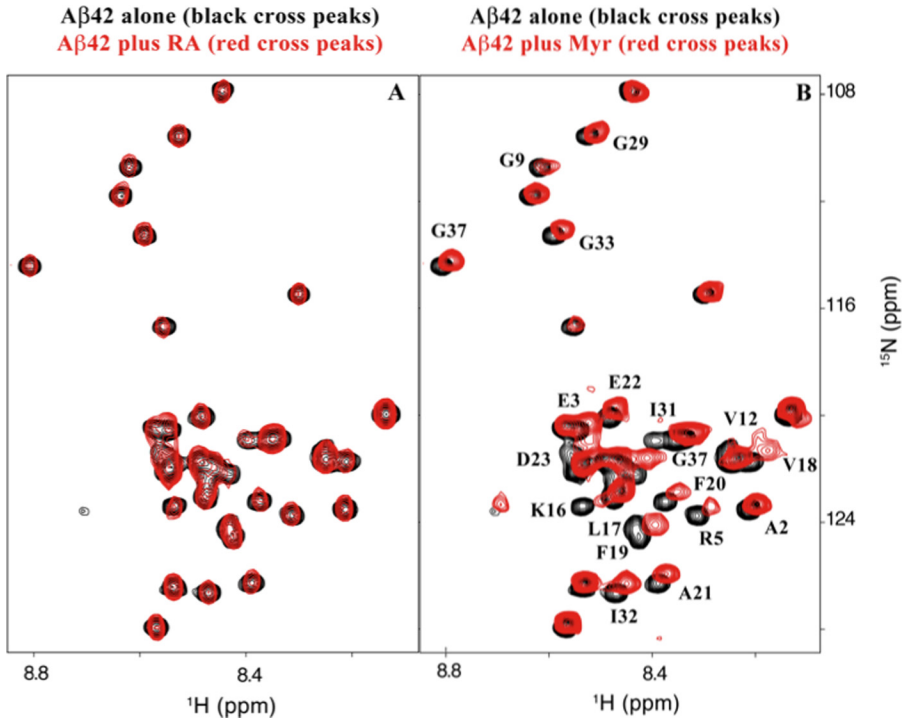

FIGURE 4. **Expanded HSQC spectra of uniformly ^{15}N-labeled Aβ42.** The HSQC experiment detects ^{1}H that are directly bonded to the ^{15}N atoms, notably the backbone amide ^{1}H-^{15}N. The control spectrum of the Aβ42 alone (25 μM, pH 7.2, 5 °C, *black cross-peaks*) is overlaid with the spectra of the Aβ42 (25 μM) containing RA (*A*) or Myr (*B*) both at 500 μM concentrations (*red cross-peaks*).

Gly-37–Ile-41. The regions showing phenol-induced chemical shifts are colored in *red* and because RA did not promote changes (Fig. 4*A*), only the green unlabeled backbone structure is shown. It is obvious that Myr causes extensive changes throughout the sequence, with continuous nine- and three-residue spans at Lys-16–Val-24 and Ile-31–Gly-33. By contrast, FA, NDGA, and Cur interactions are more limited and interestingly occur at identical residues: Arg-5, Ser-8, Gly-9, His-133, Lys-16, Asp-23, and Ile-31. (Cur also causes shifts of Leu-17.) With the exception of RA, all phenolic compounds have a proclivity for polar or charged amino acid residues.

Cellular Toxicity—The ability of Myr and RA to inhibit formation of low-*n* Aβ oligomers suggested that it might be useful in blocking the Aβ-mediated cellular toxicity. To address this possibility, we performed MTT assays (35) and probed the cellular metabolism of human embryonic kidney (HEK) 293 cells. The MTT assay constitutes a rapid and sensitive method for determination of gross Aβ toxicity in cultures of dissociated cells (36).

Previous short duration incubation experiments established that the cross-linked Aβ40 and Aβ42 oligomers were more toxic than uncross-linked oligomers (7, 23). In the present study, we explored the immediate consequences (*i.e.* no incubation time) on the viability of cells. Overall, the results are consistent with the previous study, in that uncross-linked and cross-linked Aβ42 oligomers (1 μM concentration and added immediately to the cells) showed cell viabilities of ~95 and ~79%, respectively. Thus, the cross-linked oligomers were significantly more toxic than uncross-linked oligomers ($p < 0.05$) (supplemental Fig. S6). Repeating the experiments with Myr showed almost a complete loss of cell toxicity, with the cross-linked oligomer with Myr producing slightly lower toxicity ($p < 0.05$). Using RA (instead of Myr) also reduced the toxicity to ≈ 6%, which was a major reduction relative to cross-linked Aβ42 ($p < 0.05$).

Similar observations were made in experiments with Aβ42 at higher concentrations (10 μM) (supplemental Fig. S6). Uncross-linked and cross-linked Aβ42 displayed ~53 and ~44% cell viability levels, respectively, revealing a trend toward higher toxicity with cross-linked Aβ42. Myr and RA treatment increased cell viability significantly, 69 and 64% ($p < 0.01$) higher, respectively. In summary, regardless of the cross-linked state, Myr and RA are effective in disrupting the cellular toxicity associated with low-*n* Aβ42 oligomers.

Electrophysiology—To obtain an index of Aβ42-induced functional alteration of synaptic transmission, we analyzed LTP and LTD in the CA1 region of mouse hippocampal slices. Synaptic current strength was estimated from fEPSP slope (Fig. 6, *A* and *B*). The vehicle group indicated LTP by tetanus stimulation (150 ± 6.7%). Cross-linked Aβ42 completely inhibited induction of LTP (97.5 ± 7.6%) without any alterations in baseline transmission. In contrast, cross-linked Aβ42 treated with Myr and RA induced LTP comparable with that of the vehicle alone (157 ± 5.1% and 144 ± 11.1%, respectively). Uncross-linked Aβ42 also induced LTP comparable with that in the vehicle (140 ± 10.1%). Fig. 6*C* shows differences in LTP induction among the five treatment groups. There was a significant group effect on % fEPSP slope ($F(4,22) = 6.295$, $p < 0.005$). The post hoc tests showed that % fEPSP slope in the cross-linked Aβ42 group was significantly lower than those in the other four groups (Fig. 6*C*; **, $p < 0.01$), indicating that cross-linked Aβ42

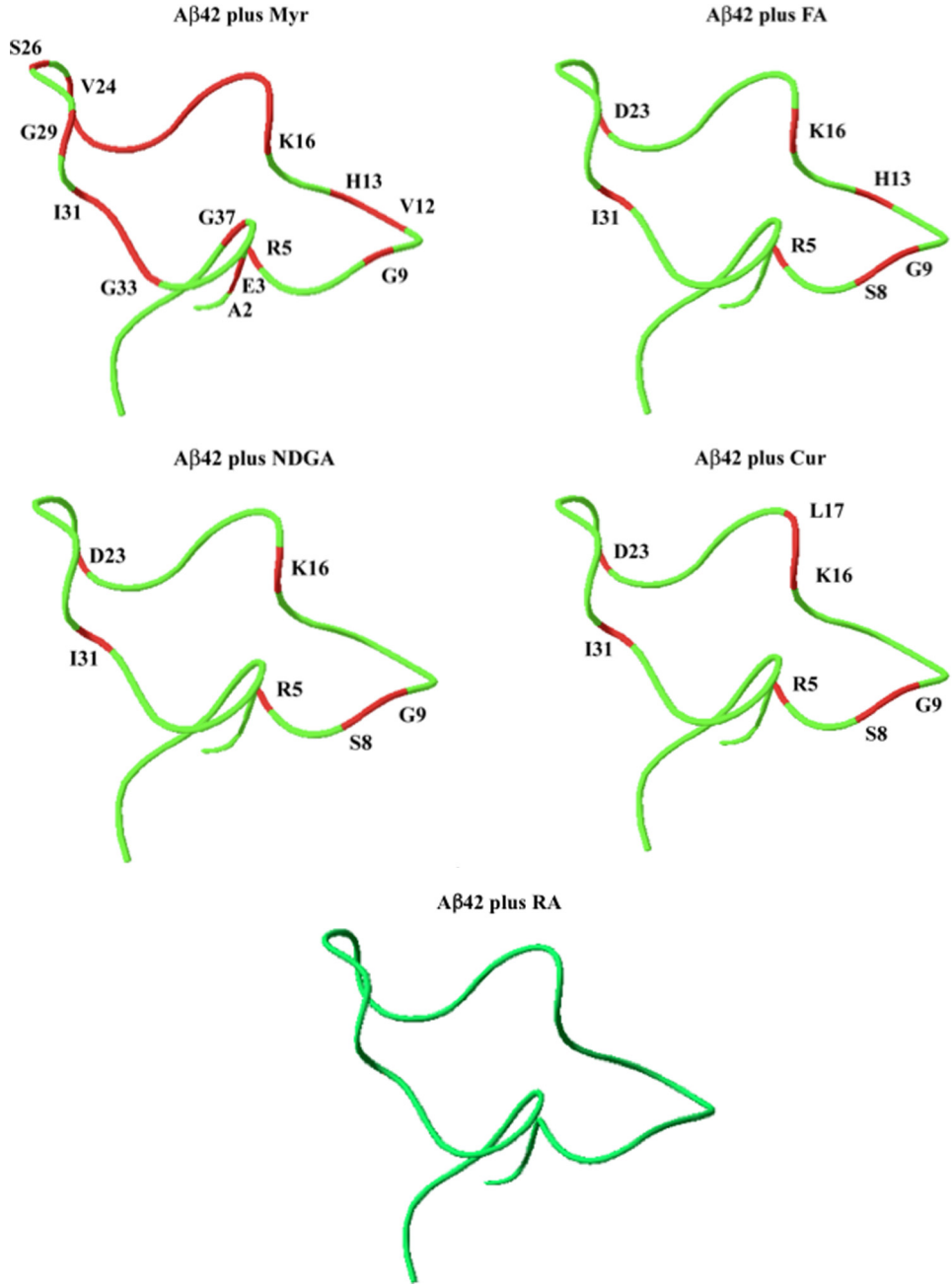

FIGURE 5. **Representative NMR/MD structural models of Aβ42 that show binding locations with the phenolic compounds.** The molecular models of the Aβ42 that were obtained from a combined molecular dynamics and NMR approach (27). The *green ribbons* depict the backbone atoms, with those regions showing chemical shift changes (indicative of binding to the phenolic compounds) are *red*. Residues at the margins of the binding regions are labeled.

induced LTP suppression, but cross-linked Aβ42 treated with Myr and RA did not.

Low frequency conditioning stimulation (1 Hz, 450 paired-pulse) induced a transient decrease in % fEPSP slope beyond the 95% lower confidence limit of the baselines in all groups (Fig. 6, *D* and *E*). This short term decrease in synaptic transmission recovered gradually, and the vehicle group showed % fEPSP slope comparable to the base-line level (104.2 ± 10.1%) during 50–60 min after LTD induction. The cross-linked Aβ42 with Myr and RA as well as uncross-linked Aβ42 groups also showed % fEPSP slopes comparable with the base-line level (102 ± 2.6, 94 ± 4.2, and 105 ± 9.4%, respectively) during 50–60 min after LTD induction. However, the cross-linked Aβ42 group showed LTD (69 ± 6.6%) by low frequency conditioning stimulation. Fig. 6*F* shows differences in LTD induction among the five treatment groups. There was a significant group effect on % fEPSP slopes ($F(4,20) = 6.925$, $p < 0.005$). The post hoc tests showed that fEPSP in the cross-linked Aβ42 group was significantly lower than that in the other four groups (Fig. 6*F*; *, $p < 0.05$; **, $p < 0.01$), indicating that cross-linked Aβ42 induced LTD facilitation but not cross-linked Aβ42 treated with Myr and RA.

DISCUSSION

We reported previously that phenolic compounds are effective *in vitro* inhibitors of fAβ formation and could destabilize

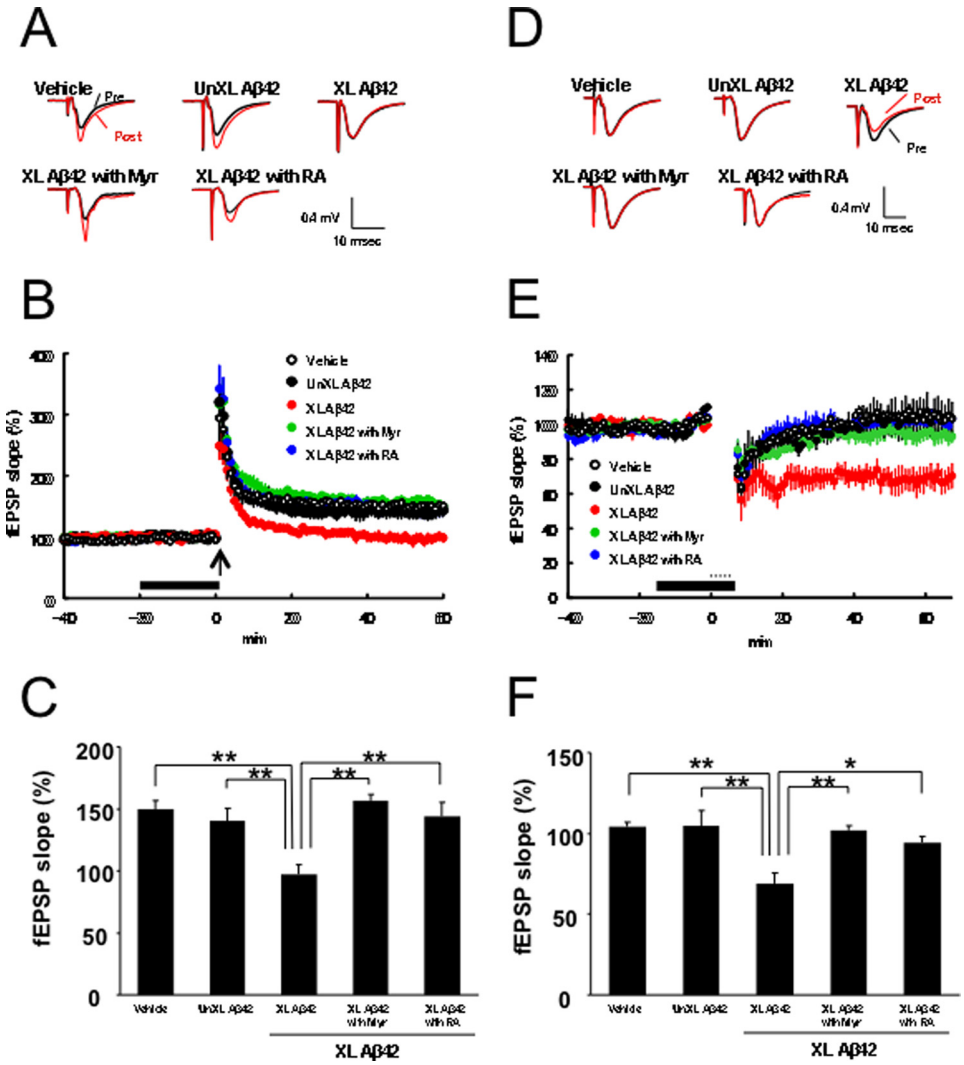

FIGURE 6. **Effects of Myr and RA on Aβ42-induced alterations of neuronal plasticity (LTP and LTD) in the hippocampal slices.** *A* and *D*, typical fEPSP waveforms of pretetanic (*black lines*) and post-tetanic (*A*) or post-low frequency (*D*) conditioning (*red lines*) stimulation in each test group. Thirty waveforms were averaged. *B* and *E*, time course of % fEPSP slope. A *thick line* indicates application of various test compounds. *B*, an *arrow* indicates tetanus stimulation (100 Hz, 1 s). *E*, *dots above the thick line* indicate low frequency conditioning stimulation (*E*, 1 Hz, 450 paired-pulse). *C* and *F*, comparison of % fEPSP slope among the five groups. Values are shown as the percentage of fEPSP slope relative to the base line and presented as mean ± S.E. ($n = 5$). Differences reaching statistical significance are noted by line segments between samples, along with their associated p values, where an *asterisk* signifies $p < 0.05$, and a *double asterisk* signifies $p < 0.01$.

preformed fAβ (14–16). Our subsequent *in vivo* work with Tg2576 mice established that Myr and RA reduced the amount of Aβ oligomers in the brain and prevented the development of AD pathology (18). The purpose of the present study was to unravel chemical and neurophysiological bases for these effects, which could accelerate the development of more effective aggregation inhibitors.

Mechanism of Polyphenol Inhibition to Amyloid Formation—Supplemental Fig. S7 presents a summary of how the polyphenols interfere with Aβ aggregation. The monomer → soluble oligomer → soluble β-sheet oligomer → protofibril → mature fibril is generally recognized as the normal "on pathway" process associated with plaque formation of the Aβ and other amyloid-forming proteins. The PICUP studies revealed that all five phenolic compounds dose-dependently inhibited Aβ40 and Aβ42 later stage oligomerization, and the PICUP method requires that monomers be in close proximity for covalent cross-linking to occur. The CD studies showed that Myr and RA stabilized Aβ populations comprising mostly random coil and inhibited statistical coils → β-sheet conversion, which was consistent with the PICUP data. However, at the atomic level, NMR showed that Myr and RA behave differently, in that Myr shows significant binding to monomeric Aβ42, whereas RA does not bind to the monomer. This result is intriguing, in that it is possible that RA could prevent aggregation by binding with non-NMR detectable early formed oligomers (dimers, trimers, etc.) (37), and in doing so prevents neurotoxicity by binding to an exposed toxic structural motif. Other Aβ binding compounds bind in a similar manner, including human serum albumin (33), apolipoprotein E3 (38), and alcohol dehydrogenase (39). Another possibility is that RA binds to distinct monomer conformers/structures that in turn inhibit oligomerization (40).

The NMR studies also established that Myr, NDGA, FA, and Cur bind to localized or specific monomeric Aβ peptide regions (Fig. 5), which are Arg-5, Ser-8, Gly-9, His-13, Lys-16, Asp-23, and Ile-31. The polyphenol (−)-epigallocatechin gallate pre-

vents α-synuclein (41) and Aβ42 aggregation by also binding to small (localized) amino acid regions. Related work (42) reported that the flavonoid baicalein stabilized a partially folded conformer of α-synuclein that existed within oligomeric assemblies. Conway *et al.* (43) showed that dopamine or levodopa inhibits the fibrillization of α-synuclein filaments, presumably through stabilization of α-synuclein into protofibrillar structures unable to form fibrils. Taniguchi *et al.* (44) reported the formation of tau oligomers in the presence of phenothiazines, polyphenols, or porphyrins. In each of these cases, the inhibitors stabilized oligomeric states, in which the respective protein maintained at least a partial fold. For Aβ, if the "oligomer cascade" hypothesis is true (2), aggregation inhibitors that stabilize oligomers could produce peptide populations of enhanced toxicity. The observation that some of the phenolic compounds bind monomeric Aβ and prevent its oligomerization is a particularly important feature.

Polyphenol Inhibition of Neuronal Toxicity and Relationship to in Vivo Studies—With our previous Tg2576 mice study (18), RA was very promising because it inhibited both high molecular weight Aβ oligomerization and Aβ deposition, whereas FA did not inhibit either process. However, our present *in vitro* studies demonstrate that all phenolic compounds (including FA) prevent low order (< 10 monomers) oligomer formation. This discrepancy could be due to the nonspecific nature of the A11 antibody that was used to detect oligomers in the Tg2576 mice (18), particularly when compared with cross-linked oligomers detected by PICUP. Similar findings were reported by Necula *et al.* (45), where dot blot assays with the A11 antibody showed that Myr, NDGA, and Cur inhibited high molecular weight Aβ oligomerization but not fibrillization.

Myr and RA decreased Aβ oligomer-induced synaptic toxicities using LTP and LTD assays of hippocampal slices. LTP and LTD are considered important neurophysiological models of memory and learning and are used as experimental models of neuronal plasticity (46). Townsend *et al.* (4) found that Aββ trimers fully inhibit LTP, whereas dimers and tetramers have an intermediate potency. Dimers and trimers from the conditioned medium of amyloid precursor protein-expressing CHO cells have been found to cause progressive loss of synapses in organotypic rat hippocampal slices (5). Aβ oligomers extracted from AD brains potently inhibited LTP and enhanced LTD, indicating disruption of synapse structure and function (6). Our present work is consistent with previous studies (4–6), where Aβ oligomers suppressed LTP and facilitated LTD induction. Both suppression of LTP and facilitation of LTD induction in the hippocampal CA1 subfield suggests that memory formation is disturbed by Aβ oligomers. In contrast, Aβ monomers resulting from reaction with phenolic compounds did not induce such effects. These findings suggest that phenolic compounds have preventive effects on Aβ-induced memory deficits. Recent work suggested that Aβ-induced inhibition of LTP was due to a decrease in density of the NR2B subunit of NMDA receptor at the postsynaptic membrane, and facilitation of LTD was ascribed to an increase in glutamate concentration at the synaptic cleft (47, 48). These studies suggest that Aβ toxicity could selectively affect these synaptic functions with usual cell functions relatively intact in brief exposure. Therefore, deficits in Aβ-induced neuronal plasticity observed in the present study might be related to early neurophysiological alterations prior to histopathological changes such as neuronal loss and brain atrophy in AD.

Alternative Mechanisms and Benefits of Polyphenol Treatment for AD—The benefits afforded by certain polyphenols to humans or in animal studies (18) may not be just from an anti-amyloid mechanism. It could happen that in some cases the polyphenols may promote Aβ$Met\text{-}35^{red} \rightarrow$ Aβ$Met\text{-}35^{ox}$ oxidation, even though we did not detect this in the present *in vitro* studies. Leong *et al.* (49) reported that dopamine could oxidize methionine of α-synuclein peptide and in the process alter the aggregation properties of the protein.

Myr has antioxidant, anti-inflammatory, anticarcinogen, and antiviral ativities (50), and can likewise act as a β-secretase inhibitor that reduces Aβ production in a cell cultures (51). FA protects neurons against Aβ-induced oxidative stress and neurotoxicity *in vitro* (52), and long term administration protects mice against Aβ-induced learning and memory deficits *in vivo*. In fact, it has been now established firmly that all polyphenols have related biological activities, most of which are beneficial *in vivo*.

Another possibility is that the polyphenols could slow down normal age-related events such as synaptic dysfunction and in doing so prevent microglial activation and attendant inflammatory responses that lead to neuronal loss and dementia (53). It is also possible that the beneficial effects may not come from the polyphenols themselves but rather from polyphenol metabolites, which can be generated by microbial enzymes in the colon (54). Once produced, these metabolites could enter the brain and reduce the inflammation associated with AD.

Conclusions—Our results established that the phenolic compounds inhibit the oligomerization and the statistical coils → β-sheet conversion of the Aβ40 and Aβ42, whereas NMR revealed possible binding interaction sites of the phenolic compounds. In addition, the MTT, LTP, and LTD assays established that the phenols inhibit Aβ oligomer-induced cellular and synaptic toxicities. Although the exact *in vivo* mechanism behind the benefits of polyphenols remains to be established, the present data, coupled with previously reported antioxidant and ameliorative effects, suggest that phenolic compounds are worthy therapeutic candidates for AD.

Acknowledgments—We thank Dr. Chunyu Wang (Rensselaer Polytechnic Institute) for providing models of the Aβ42 structures and Margaret Condron (UCLA) for technical assistance.

REFERENCES

1. Haass, C., and Selkoe, D. J. (2007) Soluble protein oligomers in neurodegeneration: Lessons from the Alzheimer amyloid β peptide. *Nat. Rev. Mol. Cell Biol.* **8,** 101–112
2. Roychaudhuri, R., Yang, M., Hoshi, M. M., and Teplow, D. B. (2009) Amyloid β protein assembly and Alzheimer disease. *J. Biol. Chem.* **284,** 4749–4753
3. Ono, K., and Yamada, M. (2011) Low-n oligomers as therapeutic targets of Alzheimer disease. *J. Neurochem.* **117,** 19–28
4. Townsend, M., Shankar, G. M., Mehta, T., Walsh, D. M., and Selkoe, D. J. (2006) Effects of secreted oligomers of amyloid β-protein on hippocampal synaptic plasticity: A potent role for trimers. *J. Physiol.* **572,** 477–492

5. Shankar, G. M., Bloodgood, B. L., Townsend, M., Walsh, D. M., Selkoe, D. J., and Sabatini, B. L. (2007) Natural oligomers of the Alzheimer amyloid-β protein induce reversible synapse loss by modulating an NMDA-type glutamate receptor-dependent signaling pathway. *J. Neurosci.* **27,** 2866–2875
6. Shankar, G. M., Li, S., Mehta, T. H., Garcia-Munoz, A., Shepardson, N. E., Smith, I., Brett, F. M., Farrell, M. A., Rowan, M. J., Lemere, C. A., Regan, C. M., Walsh, D. M., Sabatini, B. L., and Selkoe, D. J. (2008) Amyloid-β protein dimers isolated directly from Alzheimer brains impair synaptic plasticity and memory. *Nat. Med.* **14,** 837–842
7. Ono, K., Condron, M. M., and Teplow, D. B. (2009) Structure-neurotoxicity relationships of amyloid β protein oligomers. *Proc. Natl. Acad. Sci. U.S.A.* **106,** 14745–14750
8. Orgogozo, J. M., Dartigues, J. F., Lafont, S., Letenneur, L., Commenges, D., Salamon, R., Renaud, S., and Breteler, M. B. (1997) Wine consumption and dementia in the elderly: A prospective community study in the Bordeaux area. *Rev. Neurol.* **153,** 185–192
9. Truelsen, T., Thudium, D., Grønbaek, M., and Copenhagen City Heart Study (2002) Amount and type of alcohol and risk of dementia: The Copenhagen City Heart Study. *Neurology* **59,** 1313–1319
10. Flamini, R. (2003) Mass spectrometry in grape and wine chemistry. Part I: Polyphenols. *Mass Spectrom. Rev.* **22,** 218–250
11. Marambaud, P., Zhao, H., and Davies, P. (2005) Resveratrol promotes clearance of Alzheimer disease amyloid-β peptides. *J. Biol. Chem.* **280,** 37377–37382
12. Sharma, R. A., Gescher, A. J., and Steward, W. P. (2005) Curcumin: The story so far. *Eur. J. Cancer* **41,** 1955–1968
13. Ganguli, M., Chandra, V., Kamboh, M. I., Johnston, J. M., Dodge, H. H., Thelma, B. K., Juyal, R. C., Pandav, R., Belle, S. H., and DeKosky, S. T. (2000) Apolipoprotein E polymorphism and Alzheimer disease: The Indo-US Cross-national Dementia Study. *Arch. Neurol.* **57,** 824–830
14. Ono, K., Yoshiike, Y., Takashima, A., Hasegawa, K., Naiki, H., and Yamada, M. (2003) Potent anti-amyloidogenic and fibril-destabilizing effects of polyphenols *in vitro*: Implications for the prevention and therapeutics of Alzheimer disease. *J. Neurochem.* **87,** 172–181
15. Ono, K., Hasegawa, K., Naiki, H., and Yamada, M. (2004) Curcumin has potent anti-amyloidogenic effects for Alzheimer β-amyloid fibrils *in vitro*. *J. Neurosci. Res.* **75,** 742–750
16. Ono, K., Hirohata, M., and Yamada, M. (2005) Ferulic acid destabilizes preformed β-amyloid fibrils *in vitro*. *Biochem. Biophys. Res. Commun.* **336,** 444–449
17. Wang, J., Ho, L., Zhao, W., Ono, K., Rosensweig, C., Chen, L., Humala, N., Teplow, D. B., and Pasinetti, G. M. (2008) Grape-derived polyphenolics prevent Aβ oligomerization and attenuate cognitive deterioration in a mouse model of Alzheimer disease. *J. Neurosci.* **28,** 6388–6392
18. Hamaguchi, T., Ono, K., Murase, A., and Yamada, M. (2009) Phenolic compounds prevent Alzheimer pathology through different effects on the amyloid-β aggregation pathway. *Am. J. Pathol.* **175,** 2557–2565
19. Deleted in proof
20. Ono, K., Condron, M. M., Ho, L., Wang, J., Zhao, W., Pasinetti, G. M., and Teplow, D. B. (2008) Effects of grape seed-derived polyphenols on amyloid β protein self-assembly and cytotoxicity. *J. Biol. Chem.* **283,** 32176–32187
21. Hou, L., Shao, H., Zhang, Y., Li, H., Menon, N. K., Neuhaus, E. B., Brewer, J. M., Byeon, I. J., Ray, D. G., Vitek, M. P., Iwashita, T., Makula, R. A., Przybyla, A. B., and Zagorski, M. G. (2004) Solution NMR studies of the Aβ(1–40) and Aβ(1–42) peptides establish that the Met-35 oxidation state affects the mechanism of amyloid formation. *J. Am. Chem. Soc.* **126,** 1992–2005
22. Bitan, G., and Teplow, D. B. (2004) Rapid photochemical cross-linking–a new tool for studies of metastable, amyloidogenic protein assemblies. *Acc. Chem. Res.* **37,** 357–364
23. Ono, K., Condron, M. M., and Teplow, D. B. (2010) Effects of the English (H6R) and Tottori (D7N) familial Alzheimer disease mutations on amyloid β protein assembly and toxicity. *J. Biol. Chem.* **285,** 23186–23197
24. Narayanan, S., and Reif, B. (2005) Characterization of chemical exchange between soluble and aggregated states of β-amyloid by solution-state NMR upon variation of salt conditions. *Biochemistry* **44,** 1444–1452
25. Milojevic, J., Esposito, V., Das, R., and Melacini, G. (2007) Understanding the molecular basis for the inhibition of the Alzheimer Aβ-peptide oligomerization by human serum albumin using saturation transfer difference and off-resonance relaxation NMR spectroscopy. *J. Am. Chem. Soc.* **129,** 4282–4290
26. Delaglio, F., Grzesiek, S., Vuister, G. W., Zhu, G., Pfeifer, J., and Bax, A. (1995) NMRPipe: A multidimensional spectral processing system based on UNIX pipes. *J. Biomol. NMR* **6,** 277–293
27. Sgourakis, N. G., Yan, Y., McCallum, S. A., Wang, C., and Garcia, A. E. (2007) The Alzheimer peptides Aβ40 and 42 adopt distinct conformations in water: A combined MD/NMR study. *J. Mol. Biol.* **368,** 1448–1457
28. Guex, N., and Peitsch, M. C. (1997) SWISS-MODEL and the Swiss-Pdb-Viewer: An environment for comparative protein modeling. *Electrophoresis* **18,** 2714–2723
29. Soeda, Y., Tsuneki, H., Muranaka, H., Mori, N., Hosoh, S., Ichihara, Y., Kagawa, S., Wang, X., Toyooka, N., Takamura, Y., Uwano, T., Nishijo, H., Wada, T., and Sasaoka, T. (2010) The inositol phosphatase SHIP2 negatively regulates insulin/IGF-I actions implicated in neuroprotection and memory function in mouse brain. *Mol. Endocrinol.* **24,** 1965–1977
30. Bitan, G., Tarus, B., Vollers, S. S., Lashuel, H. A., Condron, M. M., Straub, J. E., and Teplow, D. B. (2003) A molecular switch in amyloid assembly: Met-35 and amyloid β protein oligomerization. *J. Am. Chem. Soc.* **125,** 15359–15365
31. Fancy, D. A., and Kodadek, T. (1999) Chemistry for the analysis of protein-protein interactions: Rapid and efficient cross-linking triggered by long wavelength light. *Proc. Natl. Acad. Sci. U.S.A.* **96,** 6020–6024
32. Yan, Y., and Wang, C. (2006) Aβ42 is more rigid than Aβ40 at the C terminus: Implications for Aβ aggregation and toxicity. *J. Mol. Biol.* **364,** 853–862
33. Milojevic, J., Raditsis, A., and Melacini, G. (2009) Human serum albumin inhibits Aβ fibrillization through a "monomer-competitor" mechanism. *Biophys. J.* **97,** 2585–2594
34. Huang, H., Milojevic, J., and Melacini, G. (2008) Analysis and optimization of saturation transfer difference NMR experiments designed to map early self-association events in amyloidogenic peptides. *J. Phys. Chem. B* **112,** 5795–5802
35. Abe, K., and Saito, H. (1998) Amyloid β protein inhibits cellular MTT reduction not by suppression of mitochondrial succinate dehydrogenase but by acceleration of MTT formazan exocytosis in cultured rat cortical astrocytes. *Neurosci. Res.* **31,** 295–305
36. Rönicke, R., Klemm, A., Meinhardt, J., Schröder, U. H., Fändrich, M., and Reymann, K. G. (2008) Aβ mediated diminution of MTT reduction–an artifact of single cell culture? *PLoS One* **3,** e3236
37. Fawzi, N. L., Ying, J., Torchia, D. A., and Clore, G. M. (2010) Kinetics of amyloid β monomer-to-oligomer exchange by NMR relaxation. *J. Am. Chem. Soc.* **132,** 9948–9951
38. Evans, K. C., Berger, E. P., Cho, C. G., Weisgraber, K. H., and Lansbury, P. T., Jr. (1995) Apolipoprotein E is a kinetic but not a thermodynamic inhibitor of amyloid formation: Implications for the pathogenesis and treatment of Alzheimer disease. *Proc. Natl. Acad. Sci. U.S.A.* **92,** 763–767
39. Yan, Y., Liu, Y., Sorci, M., Belfort, G., Lustbader, J. W., Yan, S. S., and Wang, C. (2007) Surface plasmon resonance and nuclear magnetic resonance studies of ABAD-Aβ interaction. *Biochemistry* **46,** 1724–1731
40. Rojas, A., Liwo, A., Browne, D., and Scheraga, H. A. (2010) Mechanism of fiber assembly: Treatment of Aβ peptide aggregation with a coarse-grained united-residue force field. *J. Mol. Biol.* **404,** 537–552
41. Ehrnhoefer, D. E., Bieschke, J., Boeddrich, A., Herbst, M., Masino, L., Lurz, R., Engemann, S., Pastore, A., and Wanker, E. E. (2008) EGCG redirects amyloidogenic polypeptides into unstructured, off-pathway oligomers. *Nat. Struct. Mol. Biol.* **15,** 558–566
42. Zhu, M., Rajamani, S., Kaylor, J., Han, S., Zhou, F., and Fink, A. L. (2004) The flavonoid baicalein inhibits fibrillation of α-synuclein and disaggregates existing fibrils. *J. Biol. Chem.* **279,** 26846–26857
43. Conway, K. A., Rochet, J. C., Bieganski, R. M., and Lansbury, P. T., Jr. (2001) Kinetic stabilization of the α-synuclein protofibril by a dopamine-α-synuclein adduct. *Science* **294,** 1346–1349
44. Taniguchi, S., Suzuki, N., Masuda, M., Hisanaga, S., Iwatsubo, T., Goedert, M., and Hasegawa, M. (2005) Inhibition of heparin-induced Tau filament

formation by phenothiazines, polyphenols, and porphyrins. *J. Biol. Chem.* **280,** 7614–7623
45. Necula, M., Kayed, R., Milton, S., and Glabe, C. G. (2007) Small molecule inhibitors of aggregation indicate that amyloid β oligomerization and fibrillization pathways are independent and distinct. *J. Biol. Chem.* **282,** 10311–10324
46. Martin, S. J., Grimwood, P. D., and Morris, R. G. (2000) Synaptic plasticity and memory: An evaluation of the hypothesis. *Annu. Rev. Neurosci.* **23,** 649–711
47. Snyder, E. M., Nong, Y., Almeida, C. G., Paul, S., Moran, T., Choi, E. Y., Nairn, A. C., Salter, M. W., Lombroso, P. J., Gouras, G. K., and Greengard, P. (2005) Regulation of NMDA receptor trafficking by amyloid-β. *Nat. Neurosci.* **8,** 1051–1058
48. Li, S., Hong, S., Shepardson, N. E., Walsh, D. M., Shankar, G. M., and Selkoe, D. (2009) Soluble oligomers of amyloid β protein facilitate hippocampal long term depression by disrupting neuronal glutamate uptake. *Neuron* **62,** 788–801
49. Leong, S. L., Pham, C. L., Galatis, D., Fodero-Tavoletti, M. T., Perez, K., Hill, A. F., Masters, C. L., Ali, F. E., Barnham, K. J., and Cappai, R. (2009) Formation of dopamine-mediated α-synuclein-soluble oligomers requires methionine oxidation. *Free Radic Biol. Med.* **46,** 1328–1337
50. Ong, K. C., and Khoo, H. E. (1997) Biological effects of myricetin. *Gen. Pharmacol.* **29,** 121–126
51. Shimmyo, Y., Kihara, T., Akaike, A., Niidome, T., and Sugimoto, H. (2008) Flavonols and flavones as BACE-1 inhibitors: Structure-activity relationship in cell-free, cell-based, and *in silico* studies reveal novel pharmacophore features. *Biochim. Biophys. Acta* **1780,** 819–825
52. Sultana, R., Ravagna, A., Mohmmad-Abdul, H., Calabrese, V., and Butterfield, D. A. (2005) Ferulic acid ethyl ester protects neurons against amyloid β peptide(1–42)-induced oxidative stress and neurotoxicity: Relationship to antioxidant activity. *J. Neurochem.* **92,** 749–758
53. Herrup, K. (2010) Reimagining Alzheimer disease–an age-based hypothesis. *J. Neurosci.* **30,** 16755–16762
54. Kemperman, R. A., Bolca, S., Roger, L. C., and Vaughan, E. E. (2010) Novel approaches for analyzing gut microbes and dietary polyphenols: Challenges and opportunities. *Microbiology* **156,** 3224–3231

Molecular Bases of Disease:

Phenolic Compounds Prevent Amyloid β -Protein Oligomerization and Synaptic Dysfunction by Site-specific Binding

Kenjiro Ono, Lei Li, Yusaku Takamura, Yuji Yoshiike, Lijun Zhu, Fang Han, Xian Mao, Tokuhei Ikeda, Jun-ichi Takasaki, Hisao Nishijo, Akihiko Takashima, David B. Teplow, Michael G. Zagorski and Masahito Yamada

J. Biol. Chem. 2012, 287:14631-14643.
doi: 10.1074/jbc.M111.325456 originally published online March 5, 2012